Title	Dissipation function of the first-order phase transformation in VO2 ceramics by internal-friction measurements
Author(s)	Zhang, JX; Yang, ZH; Fung, PCW
Citation	Physical Review B (Condensed Matter), 1995, v. 52 n. 1, p. 278-284
Issued Date	1995
URL	http://hdl.handle.net/10722/43295
Rights	Creative Commons: Attribution 3.0 Hong Kong License

Dissipation function of the first-order phase transformation in VO_2 ceramics by internal-friction measurements

J. X. Zhang and Z. H. Yang*
Department of Physics, Zhongshan University, Guangzhou 510275, China

P. C. W. Fung
Department of Physics, The University of Hong Kong, Hong Kong
(Received 2 March 1994)

In order to apply the concept of the dissipation function during the first-order phase transition (FOPT) in solids, we measured the internal friction Q^{-1} and shear modulus μ for a range of frequencies of polycrystalline ceramics VO_2 as the sample passed through a FOPT across the temperature range of 300–420 K. The experiment was repeated for different temperature variation rate $\dot{T}$. We have found that for each frequency, a maximum of Q^{-1} and a minimum of μ occurred at the same temperature T_p when $\dot{T}$ was kept constant. The numerical values of the dissipation function ΔG_R plus other FOPT parameters have been deduced using Q^{-1} data. The general trend of ΔG_R-T and other results are found to be consistent with known physical aspects.

I. INTRODUCTION

In the first paper of our series,[1] we derived the equation of motion of an elementary phase interface (PI) during a first-order phase transition (FOPT) of a solid sample. In fact, the explicit expressions linking the effective driving force $\Delta G'$, the dissipation function ΔG_R, and other relevant parameters have been derived. The equations of motion, as they stand, are difficult to solve in general. By applying a forced vibration on the sample, we can introduce coupling between the oscillatory stress and consequential motion of the PI. The coupling strength function $\alpha(\omega)$ is dependent on the forced oscillation frequency, the velocity of the PI, and hence the effective driving force of the FOPT. Thus keeping the sample in the FOPT while the internal friction Q^{-1} is measured at different $\dot{T}$, we can effectively add more equations to the mathematical system so that the number of unknowns balances the number of equations. In other words, our theory essentially states that the problem of the FOPT in solids can in principle be solved via suitable internal friction and shear modulus measurements.

In order to apply this theoretical approach to a realistic system, we measured the internal friction Q^{-1} and shear modulus μ of polycrystalline ceramics VO_2 while the pellet sample was undergoing a FOPT. The measurements were carried out with various frequencies of forced oscillations intermittently across the temperature range of interest (300–400 K). Using the experimental data, we report here the successful deduction of the numerical values of the dissipation function ΔG_R over a range of temperature and changing the heating rates of temperature. In the process of analysis, we were able to calculate the numerical values of two crucial parameters characteristic of the sample material VO_2. Moreover, we attempted to check the self-consistency of our result: The general trends of ΔG_R-T were found to be consistent with the known physical aspects of the FOPT.

During the FOPT, the polycrystalline sample VO_2 changes its crystalline structure from monoclinic to tetragonal around 341 K. The transformation represents also a semiconductor (high-temperature) to insulator (low-temperature) transformation.[2] (If the sample forms single crystal, the transformation is sometimes termed a metal-to-insulator transition.) In fact, the electrical resistance of our polycrystalline specimen changed sharply by 10^3 times, while that of a single-crystalline sample would change by 10^5–10^8 times.[3] The R-T hysteresis loop of our sample was also measured to check the sample characteristics. The mathematical and numerical analyses reveal that our theoretical consequence and experimental results are consistent, providing a new route to study the FOPT of solids.

The investigation of the present paper has practical implications also since VO_2 is a thermosensitive functional material and has a high potential for industrial usage.[4,5]

II. EXPERIMENTATION AND EXPERIMENTAL RESULTS

Before we prepared the pellet sample, we needed to make a VO_2 powder using the usual chemical reaction method via the following procedures:[6] (i) Deoxidizing the V_2O_5 powder by means of the "hydrochloric acid sink" approach to obtain the $VOCl_2$ solution; (ii) dripping the $VOCl_2$ solution into a NH_4CO_3 solution in a CO_2 atmosphere for protection against an undesired chemical reaction and a violent precipitation $VOCO_3$ was obtained; (iii) after filtering $VOCO_3$ from the solution in an argon atmosphere, the precipitate was heated at 350°C until we finally obtained the VO_2 powder.

This powder was then pressed into a rectangular pellet of size $\sim 2\times 5\times 60$ mm^3, which was sintered at 1050 °C for 30 min and then furnace cooled to room temperature.

0163-1829/95/52(1)/278(7)/$06.00

Since pure VO_2 is very brittle, we introduced a special treatment to strengthen the mechanical properties of the sample by simply heating it at 350 °C in air for 30 min. The surface was polished until the thickness was 1 mm. We prepared the sample in that way because we anticipated that after oxidation (in air), some V_2O_5 would have been formed on the surface and some oxygen atoms would have diffused into the interior through crystal boundaries, providing links to join up the VO_2 (brittle) granules. In fact, our x-ray-diffraction analysis revealed that there was less than 3% in volume of V_2O_5 in the polycrystals of VO_2 in the fracture cross section.[7] Such a portion of a few percent is just about appropriate as the V_2O_5 layers have a higher degree of toughness and ductility. When the whole sample was to pass through a thermal treatment, the V_2O_5 layers could relax the thermal stress of the VO_2 granules. The sample would not break after falling from a height of 2 m to the floor, and it could endure at least 50 thermal cycles in a temperature range of about 20–150 °C.[7]

In order to confirm the nature of the FOPT, a standard R-T measurement was carried out using the four-terminal method. The hysteresis graph of Fig. 1 indicates that a FOPT has taken place. The internal friction (IF) of the sample, being represented by the standard quantity Q^{-1}, was measured by a multifunction inverted torsion pendulum system (model MF/FA-1, manufactured by the Institute of Solid State Physics, Academic Sinica) in the manner described in Ref. 8. The shear modulus μ was simultaneously measured. The temperature was raised at a rate of $\dot{T}=0.25$ K/min from room temperature to about 393 K, while Q^{-1} and μ were measured under three different frequencies of forced oscillations (0.50, 1.58, and 5.00 Hz) applied alternatively. The whole process was repeated for other four temperature variation rates: 0.5, 1.0, 2.5, and 5.0 K/min. The resolution of the IF measurement was within about 1%, while that of the relative shear modulus was 0.5% and the temperature accuracy was within about ± 0.2 K. The strain amplitude of the sample was 1×10^{-5} during measurements. The temperature controller, data storage system, x-y plotter, printout set, etc., were interfaced with an IBM PC in the usual way. X-ray-diffraction analyses were performed at room temperature and also at 373 K to check the nature of the FOPT using a commercial D max-3A machine. The transformation enthalpy was measured with a Perkin-Elemer DSC-2C scanning thermal analyzer. We wish to remark here that within the temperature range of interest, there is no phase transformation for V_2O_5 and about 3% of its presence in the sample would not affect the accuracies of the relevant quantities for the VO_2 material.[7]

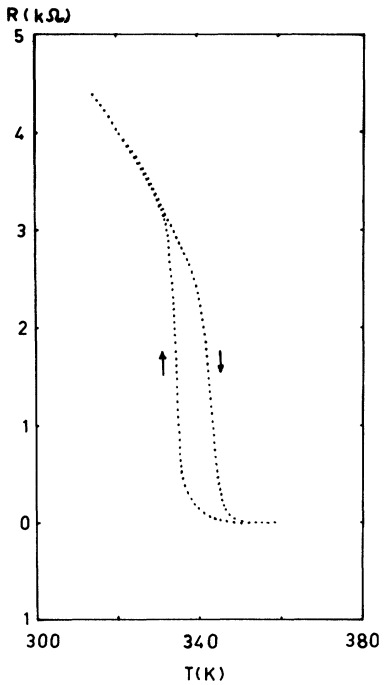

FIG. 1. Resistance R vs T of the VO_2 ceramics sample during the thermocycle of the FOPT.

Referring back to Fig. 1, we note that during the temperature ascending period, a phase transformation occurred at $T_s=331$ K and was completed at $T_f=351$ K. During the temperature descending period, a phase transformation began at $T_s'=345$ K and finished at $T_f'=327$ K. Since $T_s'>T_s$, obviously there was an overlapping region in the R-T plot during the transformation of VO_2. We must therefore adopt the definition of equilibrium temperature for thermal-elastic martensite transformations, i.e., $T_0=\frac{1}{2}(T_s+T_f')$ during the temperature ascending period and $T_0'=\frac{1}{2}(T_s'+T_f)$ during the temperature descending period.[9] Note also that there was a significant sharp change in resistance, even up to 4000 times during the transformation cycle.

X-ray-diffraction analysis at room temperature revealed that the sample had a monoclinic crystal structure, while that at 393 K had tetragonal crystal characteristics, with $a=4.55$ Å, $c=5.70$ Å. There was some tiny trace of x-ray lines pertaining to the V_2O_5 compound in the background, and a rough estimate indicated that V_2O_5 occupied less than 3% in volume of the sample. There was no indication of any significant change in the V_2O_5 lines at the two end points in temperature.[7]

Figure 2(a)–2(c) show the variations of Q^{-1} and relative shear modulus μ with respect to a change in temperature for three different heating rates $\dot{T}$ as marked. In each figure, both the Q^{-1} and μ curves for three different oscillation frequencies (0.50, 1.58, and 5.00 Hz) are shown. Inspection clearly reveals that a peak of Q^{-1} and a minimum of μ occur at the same temperature T_p; this feature is the same for all three frequencies. In each figure, we see that Q^{-1} decreases when the frequency increases. As the heating rate $\dot{T}$ is increased, we note that the amplitude of Q^{-1} increases also, with a broadening of the peak form. It is also interesting to remark that the minimum of the relative shear modulus becomes less prominent as the frequency is increased, at a fixed heating rate. Also, as $\dot{T}$ is enhanced, the minimum of the shear modulus becomes more remarkable. In the next

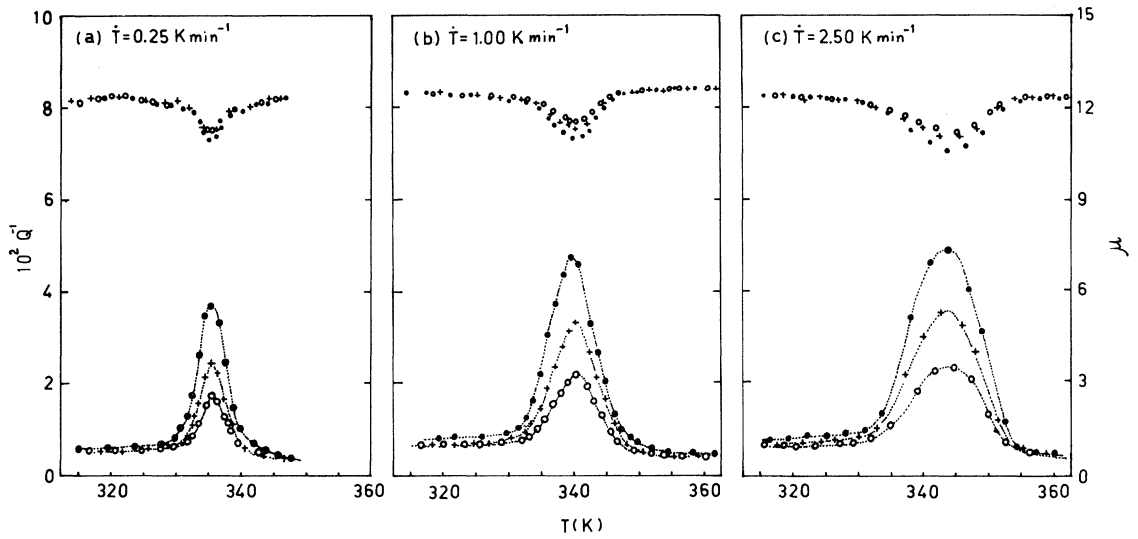

FIG. 2. Q^{-1} vs T and shear modulus M vs T of the VO_2 ceramics sample during a FOPT for (a) $\dot{T}$=0.25 K/min, (b) 1.0 K/min, and (c) 2.5 K/min.

section, we shall use the data measured to characterize the dissipation function based on the theory derived in Ref. 1.

III. CHARACTERIZATION OF THE DISSIPATION FUNCTION

The reader is referred to the details in derivation of the first paper of this series, and we highlight the important issues when necessary and simply quote here that the explicit expressions of Q^{-1} and μ and hence the (normalized) maximum relative shear modulus $\Delta\mu/\mu$:

$$Q^{-1}=Q_{\rm dyn}^{-1}+Q_0^{-1}\ , \tag{1a}$$

$$Q_0^{-1}=\alpha^2(\omega)B(T)\omega\ , \tag{1b}$$

$$Q_{\rm dyn}^{-1}=\alpha^{2(\omega)}A(T,\dot{T})(\dot{T}/\omega)^n=\alpha^2(\omega)A(F)(\dot{T}/\omega)^n\ , \tag{1c}$$

$$A(T,\dot{T})=CC'N_A(T,\dot{T})B_m\mu A_1(T,\dot{T})/(\pi\omega_0^2)$$

or

$$A(F)=CC'N_A(F)B_m\mu A_1(F)/(\pi\omega_0^2)\ , \tag{1d}$$

$$B(T,\dot{T})=2C\eta N_A(T,\dot{T})\mu/\omega_0^4$$

or

$$B(F)=2C\eta N_A(F)\mu/\omega_0^4\ , \tag{1e}$$

$$Q^{-1}\Big/\left[\frac{\Delta\mu}{\mu}\right]=f(n)\alpha(\omega)/\epsilon_0\ , \tag{2}$$

where $\alpha(\omega)$ and C' are the coupling functions describing the interaction between the PI and oscillating stress, respectively, and $N_A(T,\dot{T})$ is the total area of the moving PI per unit volume of sample. Note that N_A, A, B, and A_1 are functions of both T and $\dot{T}$. Even at a fixed T, if the sample is going through the transformation at different $\dot{T}$, then T_s, T_f corresponding to each $\dot{T}$ will not be the same and the volume fraction F of the product phase would also be different. Thus as parameters of the equation of motion, they must be evaluated at a constant volume fraction F for consistency. In (1), ω_0 is the resonant frequency of the PI, B_m and $f(n)$ are numerical coefficients arising from integration, while ϵ_0 is the strain produced by the FOPT, and η is the effective damping coefficient of the moving PI; C^{-1} is the effective mass density of the PI. Physically, $A_1(T,\dot{T})$ or $A_1(F)$ is the effective driving force coefficient, with $\Delta G'=A_1(\Delta T)^n$.

Note that $\Delta\mu/\mu$ consists of two parts: One part $(\Delta\mu/\mu)_{\rm SM}$ is associated with the softening of the phonon mode (corresponding to $\dot{T}\to 0$ and independent of $\dot{T}$), and the other part $(\Delta\mu/\mu)_{\rm PI}$ is contributed by the motion of the PI (corresponding to $\dot{T}\neq 0$). In other words,

$$y=Q^{-1}/(\Delta\mu/\mu)$$
$$=(Q_{\rm dyn}^{-1}+Q_0)\Big/\left[\left[\frac{\Delta\mu}{\mu}\right]_{\rm SM}+\left[\frac{\Delta\mu}{\mu}\right]_{\rm PI}\right]\ . \tag{3}$$

We can, in fact, obtain directly from the data of Fig. 2 the relation between y and $\dot{T}$, taking ω as the parameter for each such curve—we have three curves in Fig. 3. Clearly, at $\dot{T}=0$, $Q_{\rm dyn}^{-1}=0$, $(\Delta\mu/\mu)_{\rm PI}=0$ and the vertical intercept represents the quantity $Q_0^{-1}/(\Delta\mu/\mu)_{\rm SM}$. When $\dot{T}$ is large enough ($\sim$5 K/min), the lines in Fig. 3 approach three horizontal lines and $Q_{\rm dyn}^{-1}\gg Q_0^{-1}$, while the dependence of $(\Delta\mu/\mu)_{\rm PI}$ on $\dot{T}$ is the same as that of $Q_{\rm dyn}^{-1}$ on $\dot{T}$. Thus the vertical asymptote for each ω represents $Q_{\rm dyn}^{-1}/(\Delta\mu/\mu)_{\rm PI}$. Based on Fig. 3, it is easy to see that we can plot $\ln[Q_{\rm dyn}^{-1}/(\Delta\mu/\mu)_{\rm PI}]$ versus $\ln(\omega/\omega')$ in Fig. 4 where $\omega'=1$ Hz. Measuring the slope of the line in Fig. 4 and in view of Eq. (2), we arrive at

$$\alpha(\omega)=\alpha'\omega^{-0.2}\ , \tag{4}$$

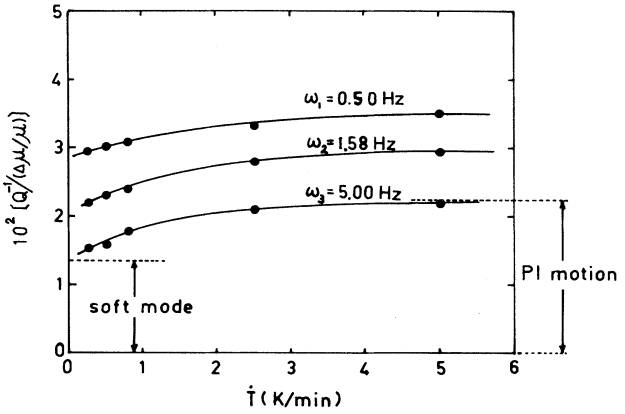

FIG. 3. $Q^{-1}/(\Delta M/M)$ vs $\dot{T}$ for the VO_2 ceramics sample.

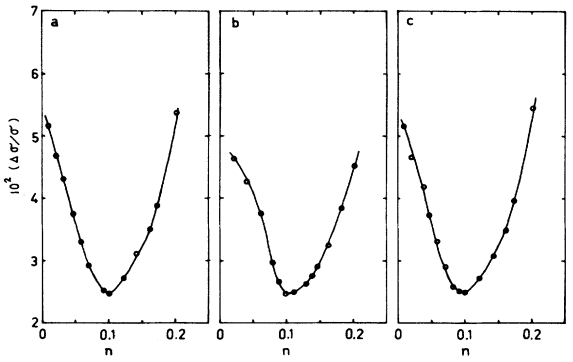

FIG. 5. rms error $\Delta\sigma/\sigma$ vs n (a) at the IF peak, (b) at $+\frac{1}{2}$ of the IF peak, and (c) at $-\frac{1}{2}$ of the IF peak.

where $\alpha' = f(n)/\epsilon_0$ is a numerical constant. Having found the functional form of the coupling function $\alpha(\omega)$, we shall proceed to find the coefficients n, $A(F)$, and $B(F)$ in (1).

From Eqs. (1) and (4) we obtain simply

$$(Q^{-1}/\omega^{0.6}) = A(F)(\dot{T}^n/\omega^{1+n}) + B(F) \; ; \qquad (5)$$

there are three ways to ensure at least approximately that the sample contains a certain fixed volume fraction at different $\dot{T}$ and T. In a phase transformation study, one usually estimates the fractional volume of the new phase at a particular T by measuring the fractional change in electrical resistance at that T. We have found experimentally that the fraction area under the Q^{-1}-T curve (in Fig. 2) at T [i.e., $\int_{T_s}^{T} Q^{-1}(T')dT' / \int_{T_s}^{T_f} Q^{-1}(T')dT'$] is equivalent to the volume fraction of the new phase as determined by electrical and differential scanning calorimetry (DSC) measurements at the same T and $\dot{T}$. On the other hand, considering a Q^{-1}-T curve for a certain $\dot{T}$, at a certain T, we can obtain a ratio $r = Q^{-1}/Q_p^{-1}$, where Q_p^{-1} is the peak value of the internal friction curve. This ratio has been found to be associated with the following physical meaning: If r for two Q^{-1}-T curves (on the same side with respect to the peak) are the same, the volume fractions of the new phase in the sample area are the same, irrespective of whatever values of $\dot{T}$ and T. For simplicity in analysis, we have taken each set of Q^{-1} data corresponding to the same r value in all the internal friction curves like those in Fig. 2; for example, we first consider $r = 0.5$, say. Then for each value of Q^{-1}, the left-hand side of (5) is fixed. We now take n as a parameter and plot $Q^{-1}/\omega^{0.6}$ against $\dot{T}^n/\omega^{1+n}$ with the available set of Q^{-1} data for each r, and calculate the root-mean-square error $\Delta\sigma/\sigma$ of the data points about the straight line which is determined by a simple least-squares fitting. Following, we plot $\Delta\sigma/\sigma$ versus n. Figures 5(a)–5(c) demonstrate that there is a minimum in each such curve for one particular ratio r [like $r = 1, \pm\frac{1}{2}$, the plus (minus) sign pertaining to the high- (low-) temperature side with respect to the peak]. Moreover, it is found that the minima of the three curves correspond to $n = 0.1$. The consistency in the value of n obtained by our analysis gives (indirect) support to the validity of the theory.

Substituting $n = 0.1$ into Eq. (5), we can find the slope $A(F)$ and intercept $B(F)$ for each r, as shown in Figs. 6(a)–6(c). It turns out that $B(F)$ is about equal to (or less

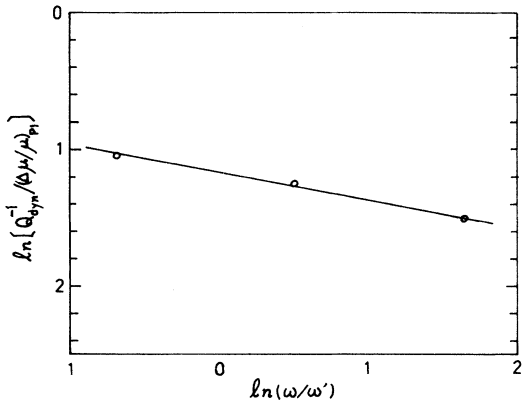

FIG. 4. Dependence of the coupling coefficient α on the frequency ω of the IF measurement.

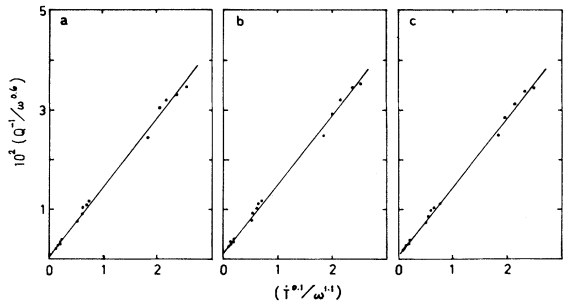

FIG. 6. (Q^{-1}/ω) vs $(\dot{T}/\omega)$ with $l = 0.2$, $n = 0.1$.

than) the background value ($\approx 4\times 10^{-4}$) in the Q^{-1}-T curves of Fig. 2, and we can assign such a numerical value to $B(F)$ or $B(T)$, as B is now practically constant for a range of T of interest.

We now turn our attention to $A(F)$. First note that for different ratios r there are different T values in general in Figs. 2(a)–2(c), since for a certain $\dot{T}$ there is a set of relations between $A(T)$ and r (or T), and we can show the $A(T)$-T relation in Fig. 7 for fixed $\dot{T}$. We obtain five such graphs from our experimental data and show only three here.

The dissipation function is expressible as

$$\Delta G_R(T)=\Delta G_d(T)-A_1(T,\dot{T})(T-T_s)^n , \tag{6a}$$

where

$$A_1(T,\dot{T})=k' A(T,\dot{T})/B(T,\dot{T}) \tag{6b}$$

and

$$k'=2\pi\eta/(C' B_m \omega_0^2) . \tag{7}$$

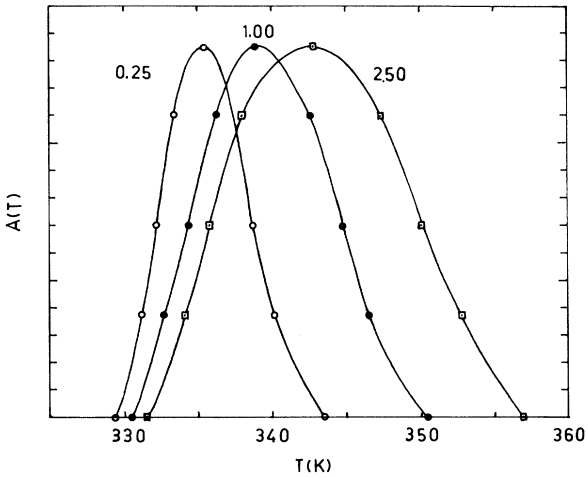

FIG. 7. $A(T)$ vs T for different $\dot{T}$.

Based on the analysis of Sec. III of Ref. 1, we learn that $\Delta G_R(T)$ has a minimum at T_v. From relation (7) and the condition $\partial[\Delta G_R(T)]/\partial T|_{T_v}=0$, k' and T_v are related by

$$k'=(\Delta H/T_0)B/\{A(T_v)(T_v-T_s)^n[d(\ln A)/dT|_{T_v}+n/(T_v-T_s)]\} . \tag{8}$$

Starting with an hypothetical value of T_v, we can calculate k' using (8) and plot the corresponding ΔG_R-T graph based on (6) with the help of the graph from which T_v is found. Putting this value of T_v into (8), again we can use an iterative process to obtain the self-consistent values of k' and T_v. Thus we can now plot ΔG_R (normalized to $\Delta H/T_0$) versus T in Fig. 8 for three different $\dot{T}$ as marked.

IV. DISCUSSION

We have noted in Ref. 1 that if the sample is in the range of the FOPT, $\Delta T=T-T_s\neq 0$, and if the FOPT is proceeding, $\dot{T}\neq 0$. When carrying out the IF experiment, surely the stress amplitude $\sigma_A\neq 0$. Under these three conditions, the interaction driving force $\Delta G_a^{\rm dyn}\neq 0$ [see Eq. (5) of Ref. 1]. The dynamic internal friction $Q_{\rm dyn}^{-1}$ is then expressible in the form (1c). It means that $Q_{\rm dyn}^{-1}$ depends on $\dot{T}$ and ω with different dependence relations according to the format $\omega^{-2l}(\dot{T}/\omega)^n=\dot{T}^n/\omega^{n+2l}$. Since $l>0$, $Q_{\rm dyn}^{-1}$ is a stronger function of $1/\omega$ than that of $\dot{T}$. We can check such a result using the experimental data of Fig. 2, and the relevant numbers are listed in Table I.

We observe that as l increases by 10 times, Q^{-1} changes from 2.44 times ($\dot{T}=0.25$ units) to 2.29 times ($\dot{T}=2.5$ units). On the other hand, as $\dot{T}$ changes by 10 times, Q^{-1} changes by only 1.35 times ($\omega=0.5$ HZ) and 1.43 times ($\omega=5.0$ Hz). We remark that we have included the first term on the right-hand side of Eq. (1a) only.

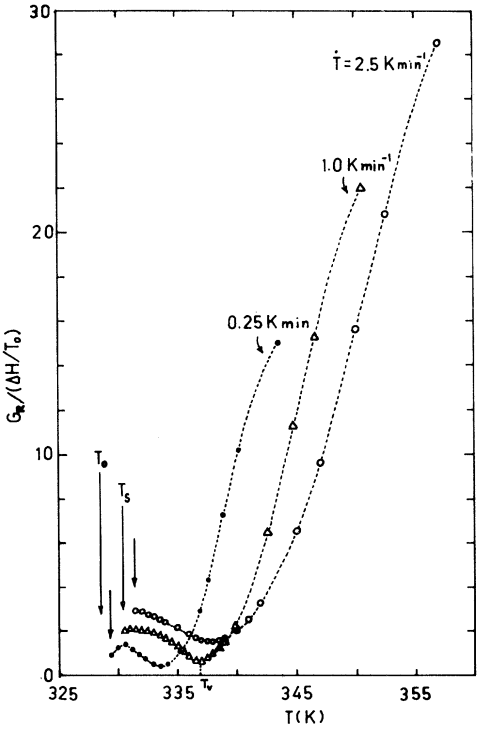

FIG. 8. Dissipation function $\Delta G_R(T)$ during a monoclinic-to-tetragonal transition.

TABLE I. Q^{-1} for various ω and $\dot{T}$ with background contributions deducted.

ω	(i)	(ii)	
$\dot{T}$	0.5 Hz	5.0 Hz	Column (i)/(ii)
(1) 0.25 K/min	3.19×10^{-2}	1.26×10^{-2}	2.44
(2) 2.50 K/min	4.33×10^{-2}	1.89×10^{-2}	2.29
Roll (2)/(1)	1.35	1.43	

If we take into account of the second term also, where $Q^{-1}=B\alpha^2(\omega)\omega=4\times10^{-4}\omega^{0.6}$, we would find that the members of the last column and last row of Table I are practically the same. The above result means that the agreement of the theory with the experimental results is excellent. This analysis shows that we need, indeed, to include the concepts of the interaction driving force $\Delta G^a_{\rm dyn}$ and coupling coefficient $\alpha(\omega,v)$ in studying the motion of the PI.

In passing, we would note that Fig. 5 depicts that n is independent of T, $\dot{T}$, or F in the VO_2 samples. Thus n is a very important index in the FOPT's of solids; it characterizes the sample material and the nature of the FOPT. It is worth noting also, from (7), that as n increases, the effective driving force increases or the dissipation of energy decreases; hence, the index n describes the dissipation of energy due to PI motion in the process of the FOPT.

(2) From expression (7), we observe that the dissipation function ΔG_R does not depend on the index l. This l is not an intrinsic parameter involved in the FOPT induced by temperature changing. It plays a different role, however. The oscillating driving force ΔG^a is expressible in terms of l (and ω) according to (4) of Ref. 1. During an IF measurement (in the presence of a FOPT), we supply heat directly to the test sample. Q^{-1} describes how much vibration energy supplied by the IF measuring system is dissipated as heat via the motion of the PI. It is natural that the coupling index l does not appear in the explicit expression of ΔG_R. If in general $v\neq0$, from Eqs. (5)–(8) of Ref. 1, we know that the coupling coefficient is expressible in various product forms:

$$\begin{aligned}\alpha(\omega,v)&\approx\alpha_0(\omega)\alpha_{\rm dyn}(v)\\&=\alpha'\omega^{-l}\alpha_{\rm dyn}(\Delta G')\\&=\alpha'\omega^{-l}C'\Delta G' .\end{aligned}$$

According to (7a), (7b), and (8), ΔG_R depends on $\Delta G'$, which depends in turn on the coupling function C'. We can see that the static coupling coefficient $\alpha_0(\omega)=\alpha'\omega^{-l}$ is related to internal friction, but not related to ΔG_R, whereas the dynamic coupling coefficient $\alpha_{\rm dyn}(v)=C'\Delta G'$ is related to both the dissipation function [see Eqs. (7a) and (8) or Eqs. (24b) and (27) in Ref. 1] and the internal friction [see Eqs. (1c) and (1d)].

(3) We shall turn to the special features of the dissipation function ΔG_R. We observe (Fig. 8) that ΔG_R-T has a minimum at $T=T_v$ in general and a relative maximum if $\dot{T}$ is relatively small. As $\dot{T}$ increases, the whole curve shifts upwards and toward a larger domain of T. Inspection of Figs. 2 and 8 leads us to conclude that $T_v<T_p$, consistent with our theoretical prediction in Ref. 1. Note that when the dissipation is minimum, the average velocity v of the PI has not yet reached its maximum. v is maximum when $T\approx T_p$, at which Q^{-1} is also maximum. Such a feature, i.e., the maximum of the effective driving force $\Delta G'$, falls behind the minimum of resistance ΔG_R, is characteristic of the FOPT, and is the origin of hysteresis in the FOPT.

When $\dot{T}$ is small, T_0 and T_s are close and the driving force $[(\Delta H/T_0)(T_s-T_0)]$ is small. During the beginning stage of the FOPT, the driving force may not be large enough to support the formation as well as the motion to the PI. A majority of the thermal energy is used in nuclei formation, and the average velocity is very small, giving rise to a peak in the dissipation as observed in our experimentation. When $\dot{T}$ is large enough, T_s becomes larger also; at sufficiently large T_s, the driving force would be large enough to cause nuclei formation and PI motion. Such an interesting aspect has been detected in Fig. 8.

(4) Based on our analysis of the VO_2 example, it appears that the theory presented in Ref. 1 can be applied to analyze the FOPT in solids, leading to the characterization of the crucial dissipation function involved. It would be fruitful to study more systems undergoing a FOPT employing such a methodology, and we hope that by understanding the general relations between n, l, and other parameters stated in item (2) of this section, a reclassification of the FOPT in solids can be introduced and a new phenomenological theory can be established.

ACKNOWLEDGMENTS

The work of J.X.Z. was supported in part by the Chinese National Science Foundation and Guangdong Province Natural Science Foundation, and in part by the Visitorship Program organized by the University of Hong Kong for Academic Staff from Universities in China and also in part by the Hsu Chung-Ching Education Foundation. P.C.W.F. is a Visiting Professor of the Physics Department, Zhong Shan University.

*Present address: Institute of Ceramics Research, Fushan, Guangdong, China.

[1]J. X. Zhang, P. C. W. Fung, and W. Geng, preceding paper, Phys. Rev. B **52**, 268 (1995).

[2]C. N. R. Ras and K. J. Ras, *Phase Transitions in Solids* (McGraw-Hill, New York, 1978).

[3]T. Mitsuishi, Appl. Phys. Lett. **40**, 89 (1982); K. L. Kavanagh, Thin Solid Films **91**, 231 (1982).

[4]M. Fukuma, Appl. Opt. **22**, 265 (1983).

[5]A. V. Salker, Thin Solid Films **150**, 11 (1987).

[6]Y. J. Luo, Acta Zhongshan Univ. **7**, 86 (1985).
[7]Z. H. Yang, Y. G. Luo, and J. X. Zhang, Prog. Mater. Sci. **5**(4), 342 (1991).
[8]J. X. Zhang, G. M. Lin, Z. C. Lin, K. F. Liang, P. C. W. Fung, and G. G. Siu, J. Phys. Condens. Matter **1**, 6939 (1989).
[9]H. C. Tong and C. M. Wayman, Acta Metall. **22**, 887 (1974); D. P. Dunne and C. M. Wayman, Metall. Trans. **4**, 137 (1973); **4**, 147 (1973).